

Improvement of Electron Recovery Using a Magnetic Field with a Low Mirror Ratio in a Secondary Electron Direct Energy Converter Simulator^{*)}

Atsuya KURISUNO, Satoshi NAKAMOTO, Kazuya ICHIMURA, Hiromasa TAKENO, Yuichi FURUYAMA¹⁾ and Akira TANIIKE¹⁾

Electrical and Electronic Engineering, Kobe University, Kobe 657-8501, Japan

¹⁾*Graduate School of Maritime Sciences, Kobe University, Kobe 658-0022, Japan*

(Received 4 January 2020 / Accepted 21 May 2020)

To recover the energy of fast protons created in D-³He fusion, a secondary electron (SE) direct energy converter was proposed, in which protons penetrated aligned metal foil electrodes, and their energy was converted into that of emitted SEs. Simulated experiments showed the problem of energy recovery of the SEs, which arose because of the magnetic mirror effect disturbing the arrival of SEs at collectors in the guiding magnetic field. To solve this problem, we propose the use of ring-type magnets to realize lower mirror ratio structures. As a result, better energy recovery is obtained for low mirror ratios because a larger part of the energy of the SEs is converted into components parallel to the magnetic field, which correspond to the direction normal to the surface of the collector.

© 2020 The Japan Society of Plasma Science and Nuclear Fusion Research

Keywords: D-³He nuclear fusion, high-energy ion, direct energy conversion, secondary electron, magnetic mirror effect

DOI: 10.1585/pfr.15.2405046

1. Introduction

In D-³He nuclear fusion reactors, most of the energy released by the reaction appears as the kinetic energy of charged particles such as electrons, thermal ions, and 14.7 MeV high-energy protons. An energy recovery device for high-energy protons, called a traveling wave direct energy converter (TWDEC), was proposed [1]; however, some protons are not decelerated, but accelerated, so the efficiency of the device is limited. Therefore, an additional device was proposed, called a secondary electron (SE) direct energy converter (SEDEC), to recover protons passing through the TWDEC [2].

An outline of the SEDEC is shown in Fig. 1. In the SEDEC, a lot of metal foil electrodes are aligned in the direction of the proton beam. The incident protons penetrate the foil electrodes, and SEs are emitted and collected by collectors located at both sides of the proton beam. Therefore, the kinetic energy of the SEs is recovered as electric power. In other words, a proton's energy can be recovered indirectly by collecting SEs.

A series of experiments on SEDEC were performed [2–5]. The magnetic field perpendicular to the beam (along the x direction in Fig. 1) was introduced to guide the SEs to collectors and not to anteroposterior foils. A magnetic field was created by a pair of permanent magnets (PMs)

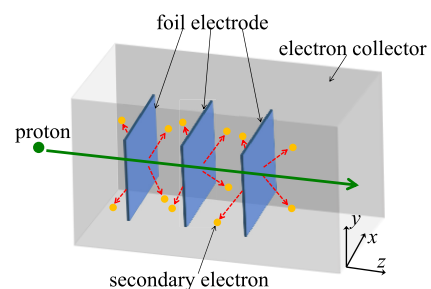


Fig. 1 Outline of the SEDEC.

behind the collector, where Fig. 2 shows the spatial distribution of the magnetic field lines. In the initial stage, small plate PMs were used (Fig. 2 (a)) where the magnetic field at the collector ($B_{\text{collector}}$) was stronger than that at the foil (B_{foil}). The SEs were subsequently reflected because of the magnetic mirror effect [3]. When we used large PMs, we can realize a mirror ratio $R_m = B_{\text{collector}}/B_{\text{foil}}$ slightly smaller than 1 to achieved better SE collection [5].

In this study, we examine the dependence of energy recovery on the mirror ratio. According to the theory of the conservation of magnetic moment, the ratio between the parallel and perpendicular (here, the directions relative to the magnetic field) kinetic energies of an electron varies in the magnetic field with the parallel gradient. In the structure shown in Fig. 2, the perpendicular energy component is not recovered as there is no electric field parallel to the

author's e-mail: takeno@eedept.kobe-u.ac.jp

^{*)} This article is based on the presentation at the 28th International Toki Conference on Plasma and Fusion Research (ITC28).

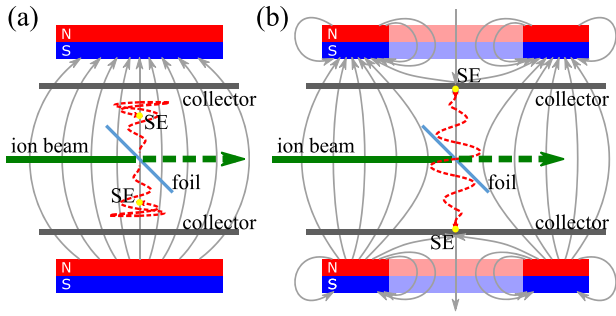


Fig. 2 Spatial distribution of magnetic field lines produced by a pair of permanent magnets of (a) plate type, (b) ring type, and location of the foil and collectors. Red broken curves are the SE's trajectories.

surface of the collector. Thus, the perpendicular energy is not useful, but the large parallel energy is advantageous for energy recovery. Thus, better energy recovery can be expected for lower mirror ratios. We examined this consideration experimentally by using ring-type PMs. A ring-type magnet originally has null points on axis, thus the distribution of field lines are as in Fig. 2 (b). This orientation allows us to obtain a small value of $B_{\text{collector}}$, i.e., $R_m \ll 1$. Moreover, we can vary R_m within 1 by changing the distance between the PMs while keeping the collectors at fixed positions. By modifying R_m , we can achieve better energy recovery for low mirror ratios.

The remainder of this study is organized as follows. In Sec. 2, the experimental setup and evaluation methods are shown. In Sec. 3, the experimental results are shown, and the discussion is presented in Sec. 4. In Sec. 5, the contents of this study are summarized.

2. Experimental Setup

A tandem electrostatic accelerator (National Electrostatics Co., 5SDH-2) was used as a high-energy proton source. The proton energy was 1.2 MeV in this study. The accelerated protons were transported to an SEDEC simulator by various orbit adjusters using electric and magnetic effects.

A schematic view of the SEDEC simulator is shown in Fig. 3. One sheet of aluminum foil, 18 μm thick, was installed in a container and electrically isolated. The center of the foil intersected the ion beam, and it was placed on axis of the ring-type PMs. The surface of the foil was orientated at 45 degrees to the ion beam and to the axis of the PMs. The container of a rectangular parallelepiped worked as a collector, where the distance between the beam and the collector was 25 mm. To prevent the ion beam from being directly incident upon the container, a shield with a hole and a back electrode were placed at the beam entrance and downstream of the beam, respectively.

A magnetic field was created by the pair of ring-type PMs. They were magnetized axially with a surface flux

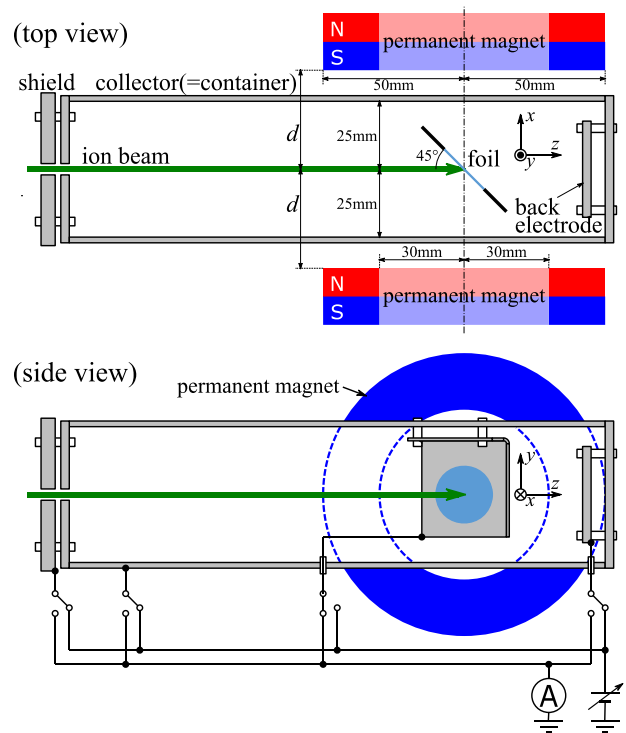


Fig. 3 Structure of the experimental SEDEC simulator.

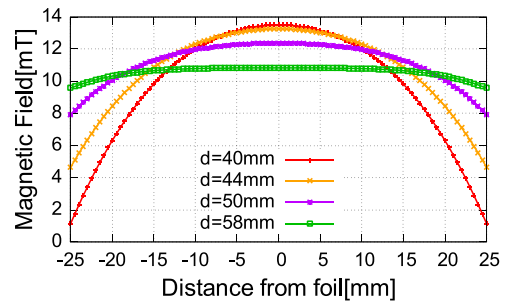


Fig. 4 Magnetic field strength between the collector plates.

density of 96 mT, and were arranged as shown in Fig. 3. They had a thickness of 20 mm, with outer and inner diameters of 100 and 60 mm, respectively. Four distances between the beam and each PM (d) were considered: $d = 40, 44, 50, 58$ mm. Figure 4 shows the calculated axial distribution of the magnetic field along the axis for each case. According to Fig. 4, we can obtain B_{foil} and $B_{\text{collector}}$ and thus R_m for each value of d ($R_m = 0.08, 0.35, 0.64, 0.88$, respectively).

The current voltage (I-V) characteristics of the foil, back electrode, and collector were measured. When making these measurements, a bias voltage was applied to all electrodes except the objective electrode. For example, the shield, back electrode, and collector were biased to measure the current of the foil electrode as displayed in Fig. 3, where “I-V characteristic of the foil” describes the relationship between the bias voltage and the measured current.

The current of the ion beam generated by the ion source varied over time. Therefore, when evaluating the characteristics of each electrode, the measured current was normalized by the current of the ion beam reaching the foil, so that the effect of the time variation of the ion beam could be taken into account. As a result, the obtained current value was measured in units of “current per 1 nA” of the incident ion beam.

3. Experimental Results

3.1 Emission of SEs

The I-V characteristics of the foil and the back electrode are shown in Fig. 5.

The measured current value represents the sum of the current of the incident ion beam and that of the SEs. As for the characteristic of the back electrode, the current was always zero, which means that the ion beam stopped at the foil and did not reach the back electrode. This is consistent with previous experiments by taking the thickness of the foil and the proton energy into account.

We further examined the characteristics of the foil. When a negative bias was applied to all electrodes except the foil, the foil formed a relatively positive potential, which caused the generated SEs to return to the foil, and hence, the net quantity of produced SEs was zero. Therefore, a saturation current in the negative bias represents the amount of ion beam, which, according to Fig. 5, is the same value as used for the normalization (i.e., 1 nA). Conversely, all SEs were emitted and did not return when a positive bias was applied. Therefore, the saturation current for a

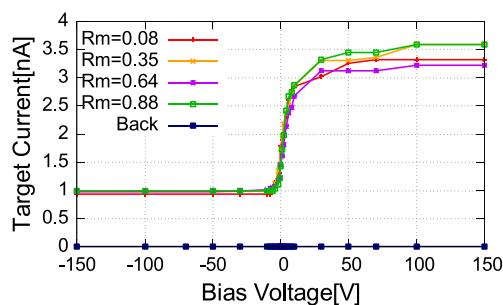


Fig. 5 I-V characteristics of the foil and back electrode.

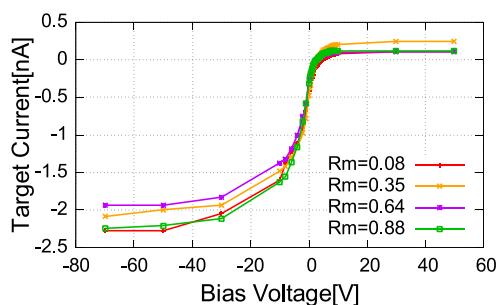


Fig. 6 I-V characteristic of the collector.

positive bias represents the sum of the current produced by all SEs emitted and that of the ion beam. Hence, the difference between the two saturation currents represents the amount of true SE emission.

According to Fig. 5, the amount of SE emission slightly changes with R_m . The cause of this variation may be due to variation of the incident angle of the ion beam and the surface condition at the incident position of the foil. Each time we changed R_m , we had to stop the operation of the accelerator, so the trajectory of the ion beam was adjusted, and the beam collimation was only done by the entrance of the collector. Although the amount of the beam is kept by the measurement and normalization, the incident beam angle and the incident point may have changed, and hence, the SE emission may also have changed [6].

3.2 Collection of SEs

The I-V characteristics of the collector are shown in Fig. 6, where the measured current represents the sum of the current due to the collected SEs and that of the scattered ions. In similar consideration to that regarding the foil, the saturation current for a positive bias (i.e., for a collector with a relatively negative potential) does not include the SEs. However, the saturation current for a negative bias does include SEs and high-energy scattered ions. If we assume that a large fraction of the scattered ions have energies higher than the saturation voltage (i.e., -70 V), the difference between the two saturation currents represents the amount of collected SEs.

According to Fig. 6, the amount of collected SEs seems to change with R_m , but it is not clear. In the next section, we will present a precise examination of this behavior.

4. Discussion

4.1 SE collection rate

We can evaluate the SE collection rate by comparing the amount of SE emission and the amount of SE collection obtained in the previous section. In Fig. 7, we have summarized the amount of SEs emitted and collected (as

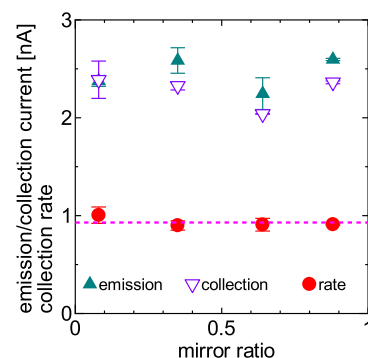


Fig. 7 Emission/collection current (triangles) and collection rate (circles) versus the mirror ratio.

currents) as a function of R_m .

According to Fig. 7, SE emission and collection change with R_m , and the collection is larger when the emission is larger. We define the collection rate by the collection current divided by the emission current, which is also shown in Fig. 7. The broken horizontal line shows the average value (0.93) of the collection rate, which is within the error ranges for all data. Thus, the collection rate does not change with R_m . According to Fig. 7, the absolute SE emission current and collection current change with R_m . This variation is not due to R_m . The emission current depends on local conditions, such as change of the incident beam angle and the incident point caused by adjustment of the beam trajectory. The collection current variations correspond to the varying emission current. Finally, most of emitted SEs are collected because of no mirror effect under the condition of $R_m < 1$.

4.2 Energy distribution of the collected SEs

The collector current I_c can be expressed by $I_c = I_i - I_e$, where I_i and I_e are the scattered ion current and SE current, respectively. The energy recovery of SEs can be achieved by a negative I_c and a positive bias (V) in Fig. 6. I_i is constant to V , so variations of I_c due to V correspond to those of I_e . Here, we examine the variation of I_e due to V .

The variation of I_e due to V arises from the energy distribution of the SEs, which can be relatively evaluated by $-dI_e(V)/dV = dI_c(V)/dV$, where the derivative can be evaluated by the finite difference of the discretely measured I_c . As a typical example, values of $R_m = 0.08$ and 0.64 are shown in Fig. 8 by symbols. To examine their decreasing tendencies, we introduced fitted functions in the form of $A \exp(-\beta V)$, where A and β are fitting coefficients. The obtained fitted functions are also shown in the figure by curves.

The obtained fitting coefficients β are shown as a function of R_m in Fig. 9. According to Fig. 9, β increases as R_m increases, which means the amount of collected SEs with high energies is relatively large for low mirror ratios. As we expected, SEs have larger parallel kinetic energies for low values of $B_{\text{collector}}$, and thus low values of R_m . The results shown in Figs. 8 and 9 are consistent with this expectation.

4.3 Energy recovery

Energy recovery is actually achieved in the conditions described by the fourth quadrant in Fig. 6. The product of the absolute value of the measured current and the bias voltage gives the recovered power. Here, the scattered ion current cancels the SE current, where this cancelation corresponds to energy lost by the energy converter. Next, we will examine the actual energy recovered, including energy losses, in a simulated experiment.

The recovered electric power versus the bias voltage

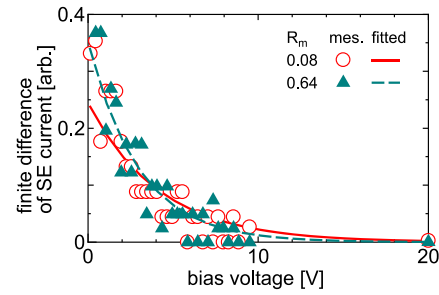


Fig. 8 Finite difference of the SE current versus the bias voltage.

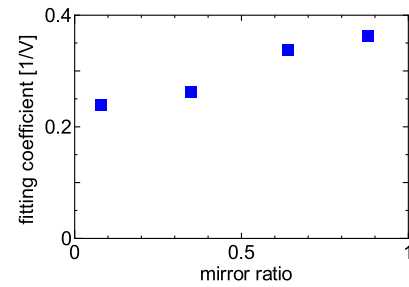


Fig. 9 Fitting coefficient versus the mirror ratio.

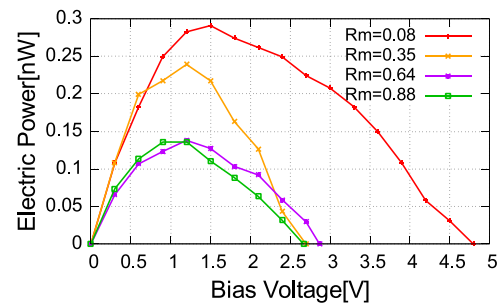


Fig. 10 Recovered electric power versus the bias voltage.

is shown in Fig. 10. According to Fig. 10, when we take an appropriate bias condition, we can maximize the electric power. The optimized powers, in the unit of nW, are 0.29, 0.24, 0.14 (0.138), and 0.14 (0.136) for $R_m = 0.08$, 0.35, 0.64, and 0.88, respectively. Larger power values are obtained for smaller mirror ratios, although the effective figures have no difference between $R_m = 0.64$ and 0.88, where translated values are different.

5. Summary

We performed simulated experiments of a SEDEC in magnetic fields with lower mirror ratios. It was found that the SE collection rate did not depend on the mirror ratio. In terms of the energy distribution of the collected SEs, a larger distribution in high-energy regions was found for lower mirror ratios, which was consistent with theoretical considerations based on the conservation of magnetic moment. As a result, better energy recovery was achieved for lower mirror ratios in the simulated experiment, and

the obtained recovery rates were 0.24×10^{-6} , 0.20×10^{-6} , 0.12×10^{-6} , and 0.11×10^{-6} , for $R_m = 0.08, 0.35, 0.64$, and 0.88 , respectively.

- [1] H. Momota, LA-11808-C, Los Alamos Natl. Lab. (1990) 8.
- [2] D. Akashi *et al.*, Trans. Fusion Sci. Technol. **63**(1T), 301 (2013).
- [3] S. Nakamoto *et al.*, Fusion Sci. Technol. **68**(1), 166 (2015).
- [4] S. Hagihara *et al.*, Plasma Fusion Res. **10**, 3405025 (2015).
- [5] A. Kurisuno *et al.*, 12th Int. Conf. on Open Magnetic Systems for Plasma Confinement (2018) P19.
- [6] T. Wada *et al.*, Plasma Fusion Res. **11**, 2405029 (2016).